Highly birefringent suspended-core photonic microcells for refractive-index sensing

Cite as: Appl. Phys. Lett. **105**, 061105 (2014); https://doi.org/10.1063/1.4892962
Submitted: 18 June 2014 . Accepted: 01 August 2014 . Published Online: 12 August 2014

Chao Wang, Wa Jin, Changrui Liao, Jun Ma, Wei Jin, Fan Yang, Hoi Lut Ho, and Yiping Wang

Highly birefringent suspended-core photonic microcells for refractive-index sensing

Chao Wang,[1,2] Wa Jin,[1] Changrui Liao,[3] Jun Ma,[1] Wei Jin,[1,a)] Fan Yang,[1] Hoi Lut Ho,[1] and Yiping Wang[3]
[1]*Department of Electrical Engineering, The Hong Kong Polytechnic University, Hong Kong, China*
[2]*The Hong Kong Polytechnic University Shenzhen Research Institute, Shenzhen 518057, China*
[3]*Key Laboratory of Optoelectronic Devices and Systems of Ministry of Education/Guangdong Province, Shenzhen University, Shenzhen 518060, China*

(Received 18 June 2014; accepted 1 August 2014; published online 12 August 2014)

An in-line photonic microcell with a highly birefringent suspended microfiber core is fabricated by locally heating and pressurizing selected air-holes of an endless single mode photonic crystal fiber. The microfiber core has rhombus-like cross-sectional geometry and could achieve a high birefringence of up to 10^{-2}. The microfiber core is fixed at the center of the microcell by thin struts attached to an outer jacket tube, which protects and isolates the microfiber from environmental contaminations. Highly sensitive and robust refractive index sensors based on such microcells are experimentally demonstrated. © *2014 AIP Publishing LLC*. [http://dx.doi.org/10.1063/1.4892962]

Optical microfibers with two-fold geometric symmetry have attracted considerable interests recently. These microfibers possess the properties of conventional circular-shaped microfiber such as strong evanescent filed, tight optical confinement, small size and light weight,[1] and at the same time exhibit high birefringence, which would enable useful applications such as highly sensitive refractive-index (RI) sensors,[2,3] optical wavelength filters,[3,4] birefringent fiber coil resonator,[5] and polarization converters.[6]

The birefringence of a microfiber is affected by the geometric aspect ratio, the size of microfiber, and the RI contrast between the core and cladding. For a microfiber with air-cladding, the birefringence gets higher with larger aspect ratio and approaches a maximum value when the cross-sectional dimension is about the wavelength-scale.[7] So far, highly birefringent (Hi-Bi) microfibers have been fabricated by tapering non-cylindrical fibers such as rectangular fiber[7,8] and D-fiber[9] or by etching cylindrical fibers with traveling micro-droplets of hydrofluoric acid.[10]

In this Letter, we report Hi-Bi microfiber with a rhombus-like cross-sectional shape. As illustrated in Fig. 1, the microfiber is housed inside a photonic microcell made by locally inflating selected air-holes[11] of a photonic crystal fiber (PCF). The two ends of the microfiber are automatically and adiabatically connected PCF pigtails from which the microcell is fabricated. The expanded holes are sufficiently large to prevent leakage of the evanescent field, while the jacket tube protects the microfiber from external contaminations and makes the device much more robust as compared with a bare air-clad microfiber. The air-region between the jacket and the microfiber provides a contamination-free platform for light-matter interaction through the evanescent field of an optical mode propagating in the suspended micro fiber core.

The fabrication of the photonic microcell follows a three-step process: At first, four air-holes at one end of the PCF, as illustrated in Fig. 2(a), are selectively opened by use of a femtosecond laser-assisted selective opening technique.[12] The other end of the PCF is spliced to a single mode fiber (SMF) to seal all the air-holes at this end. Second, high pressure gas is applied to the four selected air-columns of the PCF via the openings. Gas pressures in other air-columns remain at atmospheric pressure. Finally, the pressurized air-columns are locally inflated via a heating/tapering process.[11] During this process, the pressurized columns expand while other columns collapse gradually and eventually the central core is isolated from other part of the fiber by a large air region, with extremely thin struts which support the core.

The micrographs of a typical microcell at the suspended core region and the transition region are given in Figs. 2(b) and 2(c), respectively. The rhombus-like core (microfiber) is supported by four struts connected to the outer jacket tube and the thicknesses of the struts are thinner than 300 nm. The microfiber geometry is formed as the result of asymmetric stretching of the struts that have different thicknesses and has a high aspect ratio of ~2, exhibiting high birefringence. To minimize the loss occurring in transition, the struts with sub-wavelength width should be formed before the unpressurized air-holes are completely collapsed. This is done by controlling the gas pressure so that the expansion rate of selected air-holes is much faster than the collapsing rate of the remaining air-holes. However, if the applied pressure is

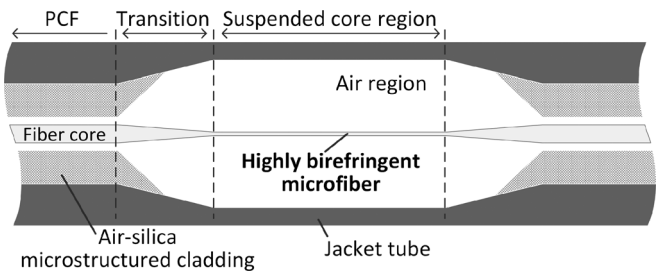

FIG. 1. Schematic of a photonic microcell with a suspended highly birefringent microfiber core.

a)Email: eewjin@polyu.edu.hk

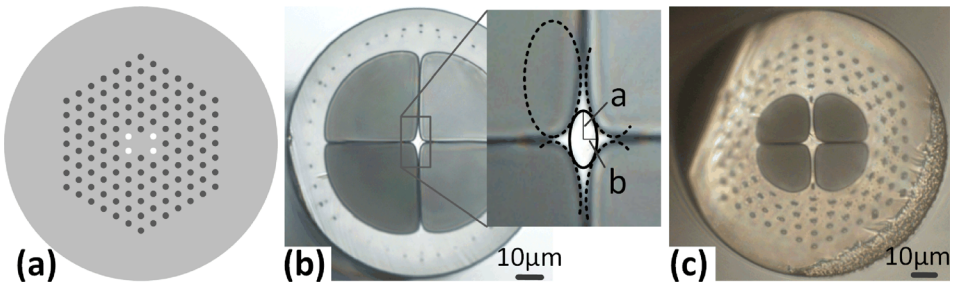

FIG. 2. (a) Schematic of photonic crystal fiber endface with four air-holes (labeled as white circles) opened for pressurization while all other air-holes are sealed. Cross-sectional micrographs of a photonic microcell with a highly birefringent (Hi-Bi) microfiber core at (b) the suspended core region and (c) the transition region. Inset of (b): model of Hi-Bi microfiber used for theoretical calculation.

too high, controlling of the expansion would become difficult, especially when the wall-thickness of the jacket tube becomes thin and high gas pressure would blow up the microcell very quickly. In our experiments, gas pressures in the range from 6 to 9 bars were used, and the insertion loss of the microcell in the wavelength range from 1250 to 1650 nm is ~0.2 dB.

The cross-sectional shape of the microfiber core may be modeled approximately by an ellipse with a long to short axis ratio of a/b = 2, as indicated in the inset of Fig. 2(b). The four curved sides of the microfiber are parts of four identical ellipses with long/short axis ratio of 2, and the minimum horizontal and vertical separations between ellipses, which correspond to the thicknesses of the struts, are set to be one-twentieth of the short and long axes, respectively. Based on this model, we numerically calculated the phase birefringence $\mathbf{B(\lambda) = |n_x(\lambda) - n_y(\lambda)|}$ by use of the COMSOL software. Here, n_x and n_y represent, respectively, the effective RI of the two polarization states of the fundamental HE_{11} mode. The calculated results are shown in Fig. 3.

In air, the Hi-Bi microfiber exhibits a theoretical maximal birefringence B_{max} of $\sim 3.5 \times 10^{-2}$ when the normalized core radius $\mathbf{r_N = r_{eq}/\lambda}$ is around 0.257, where λ is the operation wavelength and the equivalent radius r_{eq} is defined as $(a \cdot b)^{\mathbf{1/2}}$. At $\lambda = 1550$ nm, the largest birefringence $\mathbf{B_{max}}$ would be obtained when the radius r_{eq} is ~400 nm. The birefringence decreases with increasing ambient RI around the microfiber, as shown in Fig. 3(a). The peak birefringence B_{max} and the corresponding normalized core radius (r_N) as functions of n_{amb} are shown in Fig. 3(b). Based on the results in Fig. 3(a), the group birefringence **G** was calculated by using $\mathbf{G = B - \lambda \cdot (dB/d\lambda)}$ and shown in Fig. 3(c). The maximum theoretical group birefringence $\mathbf{G_{max}}$ reaches $\sim 8.2 \times 10^{-2}$ at $r_N \approx 0.19$ for $n_{amb} = 1$.

The group birefringence of the Hi-Bi microfiber was measured by use of a Sagnac loop interferometer (SLI) illustrated in Fig. 4(a). The loop coupler is a 3-dB coupler and multiple side-holes were drilled on the outer-jacket of the microcell for liquid and gas filling. A polarization controller (PC) was used in the loop to maximize the fringe contrast. Fig. 4(b) shows the measured transmission spectra of a photonic microcell with a rhombus-like microfiber core when the cell is filled with air and a RI liquid with n = 1.3. The length and the radius of the microfiber are, respectively, $\mathbf{L \approx 1\,cm}$ and $\mathbf{r_{eq} \approx 1.6\,\mu m}$. Interference fringes were observed and the fringe spacing is related to the group birefringence (G) and length (L) of the microfiber by $\mathbf{\Delta\lambda \approx |\lambda^2/G \cdot L|}$.[13]

At the wavelength of ~1550 nm, G value of the microfiber in air was determined to be $\sim 4.8 \times 10^{-3}$ and $\sim 1.5 \times 10^{-3}$ when the microcell is filled with the RI liquid. These results are in agreement with the simulation results in Fig. 3(c).

By monitoring the wavelength at one of the fringe dips as shown in Fig. 4(b), the Hi-Bi microfiber microcell may be used as a sensor to measure the RI of the surrounding material. The sensitivity (S) may be expressed as $\mathbf{S = d\lambda/dn_{amb} = (\lambda/G) \cdot (dB/dn_{amb})}$.[2] Due to the existence of G = 0 point (refer to Fig. 3(c)), the sensitivity around the sign reversing point could be significantly increased. The black and blue lines in Fig. 4(c) are, respectively, the calculated sensitivity and fringe space around the wavelength of 1550 nm as functions of microfiber radius (r_{eq}) and ambient RI (n_{amb}). The fringe space is defined as the wavelength separation between adjacent attenuation dips. For a larger n_{amb} value, the higher sensitivity region becomes broader and shifts toward larger r_{eq} values. This would allow high sensitivity RI sensors with relatively larger and practical sized

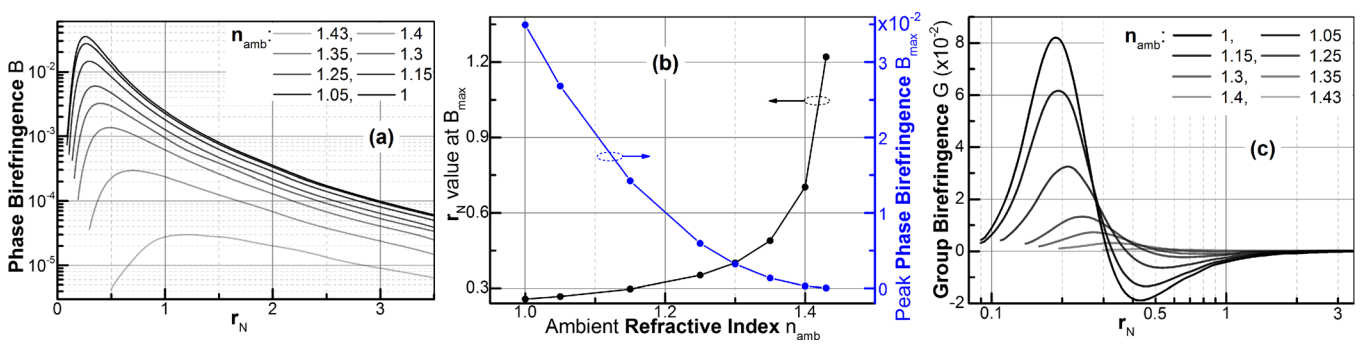

FIG. 3. (a) Calculated phase birefringence of the highly birefringent microfiber as a function of normalized core radius r_N (defined as $(a \cdot b)^{1/2}/\lambda$), for different ambient refractive index (n_{amb}). (b) Shift of birefringence peak with ambient refractive index. (c) Calculated group birefringence as a function of normalized core radius.

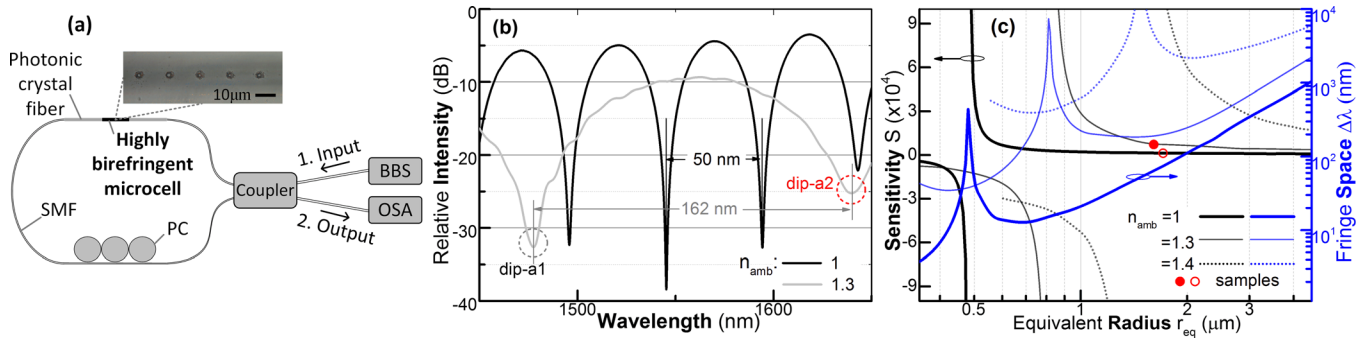

FIG. 4. (a) Experimental setup of the Sagnac loop interferometer. Inset: micrograph of the through-holes on the jacket tube of the highly birefringent (Hi-Bi) microcell. SMF: single mode fiber; PC: polarization controller; BBS: broad band source; and OSA: optical spectrum analyzer. (b) Measured transmission spectra of a Hi-Bi microfiber with ambient refractive index $n_{amb} = 1$ (black) and 1.3 (gray). (c) Calculated refractive index sensitivity (black) and fringe space (blue) around the wavelength of 1550 nm with different n_{amb}. Red dots represent samples made in experiments for refractive index sensing.

microfibers. However, the fringe space ($\Delta\lambda$) also increases with ambient RI and hence would require a longer length of microfiber to ensure at least one fringe dip is located in the operating wavelength range of the source.

The innate chambers around the Hi-Bi microfiber provide a compact and isolated space for confining small volume of sample materials and for exploiting light-matter interaction via evanescent field of the microfiber. The filling and emptying of the chambers can be achieved by the micro-channels fabricated on the jacket tube. The inset of Fig. 4(a) shows the micro-channels fabricated on the microcell by use of a femtosecond infrared laser micromachining system. As examples of potential applications, the Hi-Bi microcell which is RI-sensitive was tested for temperature and gas pressure measurement by use of the SLI set up shown in Fig. 4(a).

Temperature measurements were carried out with a liquid-filled Hi-Bi microcell with its spectra shown in Fig. 4(b). The RI liquid used was made by R. P. Cargille Lab., Inc., and has a RI of $n = 1.3$ at room temperature and a thermo-optic coefficient $dn/dt = -3.34 \times 10^{-4}/°C$. The liquid-filled sample was placed in a column oven (ECOMLCO-102) and tested from 25 to 95 °C. The wavelengths of the dips change linearly as shown in Fig. 5(a) and the dip-a2, which was always present within the wavelength range from 1450 to 1650 nm, exhibited a high temperature sensitivity of ~3 nm/°C, corresponding to a RI sensitivity of $\sim 9.1 \times 10^3$ nm/RIU. This RI sensitivity is shown as the red dot in Fig. 4(c) and agrees well with the theoretical prediction.

Measurement of gas pressure was carried out with a similar Hi-Bi microcell. The fringe spectrum of this microcell was also measured with the SLI and shown in the inset of Fig. 5(b). Eight through-holes with diameter of 3–5 μm are dilled on the microcell's jacket tube and on each strut to equalize gas pressure inside and outside the microcell. Then, the microcell was sealed inside a gas chamber made of a glass tube with bore size of ~600 μm, which was connected to a high pressure nitrogen gas cylinder via a T-tube. Pressurizing the gas within the gas chamber changes the RI of the gas[14] and results in a change in the birefringence of the microfiber. The responses of the dip wavelengths to pressure from 1 bar to 9 bars are shown in Fig. 5(b). The pressure sensitivity of the microcell is ~300 pm/bars, corresponding to a RI sensitivity of $\sim 1.5 \times 10^3$ nm/RIU. The RI sensitivity is also shown in Fig. 4(c) as the un-filled circle and agrees with the theoretical prediction. It would be possible to improve the RI sensitivity by further optimizing the dimensions of the Hi-Bi microfiber to make it closer to the maximum sensitivity point.

It should be pointed out that the Hi-Bi microcell is composed of pure silica which has a low thermo-optic coefficient[15] and the effect of temperature-induced silica RI change would have very little effect on the measurement results in Fig. 5. To verify this, we tested the temperature response of a microcell sample without material filling. The microcell was first annealed at 1000 °C for 5 h and then tested from 25 to 1000 °C. As shown in Fig. 5(c), the dip wavelength responded linearly to temperature with a very low temperature sensitivity of 3.5 pm/°C.

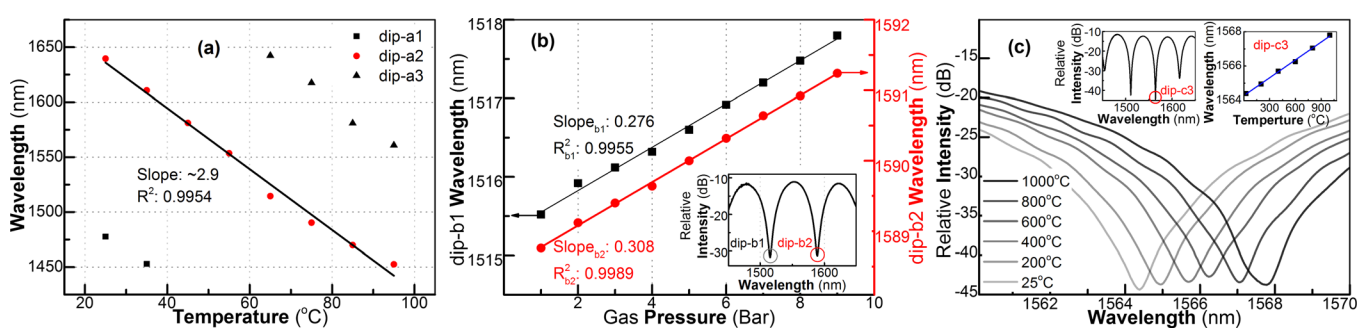

FIG. 5. (a) Measured temperature response of a highly birefringent (Hi-Bi) microcell filled with a refractive index liquid of $n = 1.3$. (b) Measured gas pressure response of a Hi-Bi microcell filled with nitrogen gas. (c) Measured temperature response of a Hi-Bi microcell without material filling (up to 1000 °C).

As compared with traditional prism-based RI sensors, optical-fiber RI sensors offer the advantages of compactness, remote detection capability, and operation in harsh environment. Different optical fiber sensors such as fiber gratings,[16,17] in-fiber cavity,[18] multimode interferometer,[19] and four-wave mixing[20] have been reported; the Hi-Bi microfiber-based sensors have demonstrated competitively high RI sensitivity ($\sim 10^4$ nm/RIU) with additional advantage of low temperature cross-sensitivity ($\sim 10^{-7}$ RIU/°C). However, the bare microfiber-based devices are vulnerable to contamination[21] and not easy to handle. The current microcell technology provides a way for embedding a Hi-Bi microfiber within an enclosed compartment and overcomes the problems associated with the use of optical microfibers. Furthermore, the tiny in-fiber cavity surrounding the microfiber provides a good platform for strong light-matter interaction in a reduced space-scale, which would be useful for nanoliter-volume spectroscopy[22] and bio-chemistry sensing.[23]

In conclusion, a Hi-Bi rhombus-like-shaped microfiber was fabricated and examined theoretically and experimentally. The microfiber is embedded inside a jacket tube to form a photonic microcell and adiabatically connects to PCF pigtails at both ends. The birefringence of such microfiber could reach up to the order of 10^{-2} and exhibits high sensitivity to ambient RI and low sensitivity to temperature. Such photonic microcells are compact and robust, have low loss, and are ideal platforms for sensors and functionalized in-fiber devices. Based on such microcells, RI, temperature, and gas pressure sensors are experimentally demonstrated, and the RI sensitivity is $\sim 10^4$ nm/RIU around $n = 1.3$.

This work was supported by the Natural Science Fundament of China (Grant No. 61290313) and the Hong Kong Polytechnic University (Grant No. G-YK62).

[1]L. Tong, F. Zi, X. Guo, and J. Lou, Opt. Commun. **285**(23), 4641 (2012).
[2]J. Li, L.-P. Sun, S. Gao, Z. Quan, Y.-L. Chang, Y. Ran, L. Jin, and B.-O. Guan, Opt. Lett. **36**(18), 3593 (2011).
[3]W. Jin, C. Wang, H. Xuan, and W. Jin, Opt. Lett. **38**(21), 4227 (2013).
[4]W. Jin, H. Xuan, and W. Jin, Opt. Lett. **39**(12), 3363 (2014).
[5]T. Lee, N. G. R. Broderick, and G. Brambilla, Opt. Commun. **284**(7), 1837 (2011).
[6]H. Xuan, J. Ma, W. Jin, and W. Jin, Opt. Express **22**(3), 3648 (2014).
[7]H. F. Xuan, J. Ju, and W. Jin, Opt. Express **18**(4), 3828 (2010).
[8]Y. Jung, G. Brambilla, K. Oh, and D. J. Richardson, Opt. Lett. **35**(3), 378 (2010).
[9]F. Beltrán-Mejía, J. H. Osório, C. R. Biazoli, and C. M. B. Cordeiro, J. Lightwave Technol. **31**(16), 2756 (2013).
[10]J. C. Mikkelsen and J. K. S. Poon, Opt. Lett. **37**(13), 2601 (2012).
[11]C. Wang, W. Jin, J. Ma, Y. Wang, H. Lut Ho, and X. Shi, Opt. Lett. **38**(11), 1881 (2013).
[12]J. Ju, H. Feng Xuan, W. Jin, S. Liu, and H. Lut Ho, Opt. Lett. **35**(23), 3886 (2010).
[13]M. Antkowiak, R. Kotynski, T. Nasilowski, P. Lesiak, J. Wojcik, W. Urbanczyk, F. Berghmans, and H. Thienpont, J. Opt. A: Pure Appl. Opt. **7**(12), 763 (2005).
[14]E. R. Peck and B. N. Khanna, J. Opt. Soc. Am. **56**(8), 1059 (1966).
[15]M. J. Weber, *Handbook of Optical Materials* (CRC Press LLC, 2002).
[16]W. Liang, Y. Huang, Y. Xu, R. K. Lee, and A. Yariv, Appl. Phys. Lett. **86**(15), 151122 (2005).
[17]L. Rindorf and O. Bang, Opt. Lett. **33**(6), 563 (2008).
[18]C. R. Liao, T. Y. Hu, and D. N. Wang, Opt. Express **20**(20), 22813 (2012).
[19]C. Li, S.-J. Qiu, Y. Chen, F. Xu, and Y.-Q. Lu, IEEE Photonics Technol. Lett. **24**(19), 1771 (2012).
[20]M. H. Frosz, A. Stefani, and O. Bang, Opt. Express **19**(11), 10471 (2011).
[21]M. Fujiwara, K. Toubaru, and S. Takeuchi, Opt. Express **19**(9), 8596 (2011).
[22]Y. Cao, W. Jin, L. Hoi Ho, and Z. Liu, Opt. Lett. **37**(2), 214 (2012).
[23]S. Heng, M.-C. Nguyen, R. Kostecki, T. M. Monro, and A. D. Abell, RSC Adv. **3**, 8308 (2013).